https://doi.org/10.5194/egusphere-2026-2192
Preprint. Discussion started: 20 May 2026

Uncovering the Functional Roles of Plasma Membrane Proteins in Foraminiferal biocalcification

Elisa Costanzi[1,6], Francesca Zito[2], Annachiara Bartolini[3], Arul Marie[4], Sylvain Bernard[5], Anna Sabbatini[6]

[1]University School for Advanced Studies IUSS Pavia, Pavia, 27100, Italy
[2]Université Paris Cité, CNRS, Biochimie des Proteines Membranaires, Paris, F-75005, France
[3]Department of Origins and Evolution, Center for Research on Palaeontology (CR2P), UMR 7207, Muséum National d'Histoire Naturelle, CNRS, Sorbonne Université, CP38, Paris, 75005, France
[4]Plateforme de spectrométrie de masse bio-organique, UMR 7245, Bâtiment 54, Allée des Crapauds, Muséum National d'Histoire Naturelle, Paris, 75005, France
[5]Institut de Minéralogie, de Physique des Matériaux et de Cosmochimie (IMPMC), UMR 7590, CNRS, Muséum National d'Histoire Naturelle, Sorbonne Université, Paris,75005, France
[6]Department of Life and Environmental Sciences, Polytechnic University of Marche, Ancona, 60131, Italy

Correspondence to: Anna Sabbatini (a.sabbatini@univpm.it), Francesca Zito (zito@ibpc.fr)

Abstract. The biocalcifying process in foraminifera, especially in benthic rotaliids like the *Ammonia* genus, involves intricate interactions between organic components and inorganic crystal formation, in which cellular membranes likely play a central but still underappreciated role.

We established a new extraction protocol enabling the isolation of membrane–associated and cytoplasmic proteins, as confirmed by proteomic analyses, revealing a clear spatial separation of protein functions. In particular, biochemical studies have identified an Annexin A13-like protein in membrane extracts of *Ammonia* spp. specimens, pointing to a conserved role for annexins in calcium regulation across diverse organisms, including these protists.

This study identifies membrane-associated proteins whose functions are likely linked to foraminiferal shell formation, potentially involving (i) annexin-mediated calcium transport at the site of biocalcification and (ii) regulation of ion flux through vesicle-based transport. Finally, we examined the Primary Organic Sheet (POS) using *in situ* carbon K-edge XANES spectroscopy on a focused ion beam (FIB) lamella from the final chamber of the *Ammonia confertitesta* test. The detection of lipid components suggests that this organic shell layer may partly derive from the plasma membrane, indicating its contribution to molecules forming the POS structure and composition.

Taken together, biochemical, proteomic, and ultrastructural evidence indicate that the plasma membrane, in addition to the well-established role of the shell organic layers, may play an active and sustained role in regulating foraminiferal biomineralization. These findings complete published models of foraminiferal biocalcification and support a framework in which the membrane and its associated proteins may represent central players in shell formation.

https://doi.org/10.5194/egusphere-2026-2192
Preprint. Discussion started: 20 May 2026

1 Introduction

Biomineralization is a biologically controlled process through which organisms regulate the deposition of inorganic minerals into complex architectures using organic matrices as templates and regulators of crystal growth. Foraminifera, single-celled eukaryotes that construct intricate mineralized tests (shells), exemplify this process with remarkable efficiency (Hemleben et al. 1977; Bè et al. 1979; Angell 1979; Angell 1980; Erez 2003; Weiner & Dove 2003; Nagai, Uematsu, Wani, et al. 2018; Geerken et al. 2019). Throughout their evolutionary history, they have developed diverse biomineralization strategies, resulting in an extraordinary array of test morphologies and compositions (Pawlowski & Holzmann 2002).

Foraminiferal biocalcification has traditionally been investigated using geochemical approaches, particularly isotopic and trace-element analyses applied to paleoenvironmental and paleoceanographic reconstructions (Katz et al. 2010; de Nooijer et al. 2014; Schiebel & Hemleben 2017; Fehrenbacher et al. 2024). However, biominerals are not passive environmental recorders but the result of tightly regulated biological processes, making it essential to understand the cellular mechanisms controlling calcification for the correct interpretation of foraminiferal proxies (Urey et al. 1951; Glas et al. 2012; de Nooijer et al. 2014; Dubicka et al. 2023).

Our study focuses on the calcifying order Rotaliida (Lankester, 1885), which includes both benthic and planktonic species and represents the most diverse and ecologically significant group of modern foraminifera. Their biocalcification processes control both the geochemical signals recorded in the test and the morphological diversity observed within the group (Toyofuku et al. 2011; Nehrke et al. 2013; van Dijk et al. 2017; Nagai, Uematsu, Chen, et al. 2018; Nagai, Uematsu, Wani, et al. 2018). Central to wall formation is the Primary Organic Sheet (POS) (Erez 2003), previously called Primary Organic Membrane (Hemleben et al. 1977). The POS (= POM) acts as a template for $CaCO_3$ precipitation during chamber formation, with associated organic layers regulating ion transport and excluding metabolic waste (Angell 1967; Angell 1979; Banner et al. 1973; Bè et al. 1979; Erez 2003; Nagai, Uematsu, Chen, et al. 2018; Nagai, Uematsu, Wani, et al. 2018). Once described as a spongy nucleation surface (Hemleben et al. 1977; Hottinger 1986), it is now interpreted as originating from dynamic pseudopodial networks that establish the site of calcification (SOC), a biologically controlled microenvironment for mineral nucleation (Nagai, Uematsu, Chen, et al. 2018; Nagai, Uematsu, Wani, et al. 2018; Tyszka et al. 2019). Despite detailed structural descriptions, the biochemical composition of the POS and associated organic layers remains poorly constrained. Available evidence suggests that these layers contain proteins, glycoproteins, and polysaccharides similar to those found in the organic matrices of other biomineralizing organisms (Weiner & Addadi 1997). Proteomic studies are therefore critical to better characterize the molecular machinery underlying foraminiferal biomineralization, yet they remain relatively limited compared to those on other marine calcifiers such as corals and mollusks. One of the key questions concerning foraminiferal biocalcification processes is how calcium cations (Ca^{2+}) are transported from the surrounding seawater to the calcification site. Several scenarios have been published in the literature: (i) uptake of calcium via seawater endocytosis, followed by transport to the calcification site by vesicles (Erez, 2003; Bentov et al., 2009; de Nooijer et al., 2009); (ii) calcium is transported to the site of calcification across the cell membrane (Nehrke et al., 2013); (iii) high-Mg Amorphous Calcium Carbonate (Mg-ACC) nano-particles are

https://doi.org/10.5194/egusphere-2026-2192
Preprint. Discussion started: 20 May 2026

bioprecipitated in intracellular vesicles by modifying seawater (e.g. increasing pH) and then transported to the site of chamber construction, supporting an alternative vesicle-mediated pathway for biocalcification (Dubicka et al. 2023, 2025). Recent work identified hundreds of test-associated proteins in *Amphistegina lobifera* involved in Ca^{2+} regulation and vesicle trafficking, supporting intracellular control on test composition (Prada et al. 2024). In this context, our approach is to isolate foraminiferal membrane-associated proteins to highlight their role in the biomineralization. To investigate this possibility, we isolated thousands of living specimens of *Ammonia* spp. and developed a protocol to separate membrane-associated and soluble proteins. Immunoblot analyses were used to track annexins, a family of Ca^{2+}-dependent phospholipid-binding proteins known to regulate membrane-related processes and considered potential regulators of biomineralization. Targeted proteomic analyses were then performed on each protein fraction to characterize the membrane proteome and identify candidate proteins potentially involved in shell formation.

Finally, we analyzed the POS using *in situ* X-ray absorption near-edge structure (XANES) spectroscopy at the carbon K-edge on a focused ion beam (FIB) lamella extracted from the final chamber of *Ammonia confertitesta* Zheng, 1978. The detection of lipid components within the POS suggests that this spongy organic layer may derive, at least in part, from the plasma membrane, providing evidence that membrane-derived molecules contribute to the structure and composition of the POS.

Taken together, these biochemical, proteomic, and ultrastructural observations indicate that the plasma membrane and its associated proteins may play an active role in regulating foraminiferal biomineralization. This perspective complements published models of biocalcification and supports a framework in which membrane processes represent key components of shell formation.

2 Materials and Methods

2.1 Foraminifera from laboratory cultures

Surface sediment samples were collected from the intertidal zone of Esnandes (Atlantic coast, France) in February 2024. Foraminiferal cultures were set up from the sediment at the Laboratory of Paleontology of the Muséum national d'Histoire naturelle (MNHN) of Paris, following the protocol described by (Caridi et al. 2020). This step was necessary to obtain and maintain live specimens for subsequent experimental purposes. After a day of acclimatisation, the sediment was sieved using a 90 µm mesh to isolate adult specimens and exclude juvenile forms, which could bias the taxonomic identification. Living specimens of *Ammonia confertitesta* Zheng, 1978 and *Ammonia parkinsoniana* (D'Orbigny, 1839) and *Ammonia tepida* (Cushman, 1926*)* were picked from the residue and observed under the stereomicroscope Leica M165C to check their vitality, assessed by the presence of sediment particles close to the aperture and/or yellow/brown colour. These two species, referred to collectively as *Ammonia* spp. throughout this study are ubiquitous and commonly found in sheltered, shallow intertidal marine environments, and sometimes in brackish waters (Walton & Sloan., 1990). *Ammonia confertitesta* is a highly competitive non-indigenous species (NIS) in Europe, first described in 2019 from France. Its distribution ranges along the NE Atlantic coast, from the Baie de l'Aiguillon to the Baltic Sea (Pavard et al., 2023). Live individuals were then isolated in

https://doi.org/10.5194/egusphere-2026-2192
Preprint. Discussion started: 20 May 2026

eppendorf tubes, and frozen at -80°C to ensure maintenance of the target structures. A subset of foraminiferal specimens was selected for imaging using Scanning Electron Microscopy (SEM, FEG TESCAN CLARA) at Electron Microscopy Platform of MNHN) to further investigate their morphological and structural features.

2.2 Protein extraction

Modifications were made to the protein extraction protocol described in (Betti et al. 2021) to obtain, from a single extraction procedure, three protein residues: total proteins, soluble proteins and membrane proteins.

After transferring 200 specimens to an eppendorf, removing excess water (aided by rapid centrifuge cycles) and treating with liquid nitrogen using an immersion bath, the tube contents were subjected to crushing with a tube pestle. The sample was homogenized with 200 µl of lysis buffer [50 mM Tris HCL, pH 8, 5 mM EDTA, pH 8, 0,25 M Sucrose, 10 mM NaF] and 2 µl of Protease Inhibitor Cocktail (100x). The homogenate sample was divided into two aliquots of 100 µl. In the first aliquot, SDS and Triton 100 to 1% were added; the resulting sample was sonicated for 45 s at 100W on ice. The sample was boiled for 10 min at 95°C and then centrifuged for 20 min at 14,000 g to remove insoluble debris, and the supernatant was recovered (total proteins).

The second aliquot was centrifuged for 20 min at 14,000 g to remove insoluble debris and the supernatant was recovered (cytoplasmic proteins). The insoluble debris was homogenized with 100 µl of lysis buffer, 1 µl of protease inhibitor cocktail (100x), SDS and Triton 100 to 1%; the obtained sample was sonicated for 45 s at 100W on ice. The samples were boiled for 10 min at 95°C and then centrifuged for 20 min at 14,000 g to remove insoluble debris, and the supernatant was recovered (membrane-associated proteins).

To each of the three samples (total proteins, soluble proteins, and membrane-associated proteins), 25 µl of Laemmli Buffer 5x was added and then the samples were heated for 1 min at 95°C.

2.3 SDS-PAGE and Western Blotting

Gel electrophoresis was carried out on NuPAGE™ 12%, Bis-Tris, 1.0 mm, Mini Protein Gels (NuPAGE® precast gel, Invitrogen) using standard SDS-PAGE techniques. Proteins were stained with the standard Coomassie Blue method.

The proteins contained in each of the three residues (total, soluble, and membrane-associated) were then analyzed by western blot using standard SDS-PAGE techniques and transferred to nitrocellulose membranes (Amersham™ Protran™ Premium 0.2µm Nitrocellulose Membranes, Cytiva). The membrane was blocked in Phosphate Buffered Saline-Tween (0,2%) (PBS-T) containing 2% Bovine serum Albumin (BSA) for 2 hours. The membrane was then incubated with the primary antibody (Anti-Annexin-13 / ANXA13 Antibody (A89469) or ANXA6 Antibody (A14725), Antibodies.com) in PBS-T (0,2%) 2% BSA, diluted 1:2000. After overnight incubation, the membranes were washed 3x PBS-T (0,2%) for 15 min each, then incubated with horseradish peroxidase-conjugated secondary antibody (Goat Anti-Rabbit IgG H&L Antibody (HRP) (A17345) Antibodies.com).

https://doi.org/10.5194/egusphere-2026-2192
Preprint. Discussion started: 20 May 2026

2.4 Sample preparation for mass spectrometry and Tryptic digestion of in-gel proteins for mass spectrometry analysis

Sample preparation for mass spectrometry analysis followed the same protocol described for protein extraction, but a larger number of individuals (500 specimens) was used to obtain a more concentrated protein extract. Gel electrophoresis was carried out on NuPAGE™ 12%, Bis-Tris, 1.0 mm, Mini Protein Gels (NuPAGE® precast gel, Invitrogen) using standard SDS-PAGE techniques, and proteins were stained with the standard Coomassie Blue method.

To remove the dye, the polyacrylamide gel pieces were treated with a series of solutions. First, 200 µl of H_2O Milli-Q® was added, and the mixture was shaken for 10 min at room temperature. The supernatant was then removed, and 200 µl of NH_4HCO_3 25 mM/50% Acetonitrile (ACN) was added, followed by shaking for 10 min at room temperature. After removing the supernatant, 200 µl of 100% ACN was added, and the mixture was shaken for 10 min at room temperature. Finally, the sample was dried in a speedvac for 4 min at 30°C in V-AQ mode.

To perform alkylation and reduction, 50 µl of 10 mM DTT/25 mM NH_4HCO_3 was added to the sample, and it was heated for 1 h at 56°C. After removing the supernatant, it was replaced with 50 µl of 55 mM iodoacetamide/25 mM NH_4HCO_3, and the sample was incubated for 45 min in the dark. The supernatant was then replaced with 100 µl of 25 mM NH_4HCO_3, and the mixture was shaken at room temperature for 10 min. After removing the supernatant, it was replaced with 100 µl of 25 mM NH_4HCO_3/50% ACN, and the mixture was shaken for 10 min at room temperature. Finally, the supernatant was removed, and the sample was replaced with 100 µl of 100% ACN, and shaken for 10 min at room temperature. The supernatant was removed, and the sample was dried in a speedvac for 4 min at 30°C in V-AQ mode.

To carry out trypsin digestion, a trypsin solution was prepared using 2 µl of Promega Gold trypsin, 50 µl of 50 mM NH_4HCO_3, 44 µl of H_2O Milli-Q®, and 4 µl of $CaCl_2$. The samples were rehydrated in 10 µl of trypsin solution on ice. Afterwards, 20–40 µl of 25 mM NH_4HCO_3 was added to cover the gel pieces, and the mixture was incubated overnight at 37°C.

The supernatant was then transferred to a new, clean tube. To extract the peptides from the gel, 35 µl of 50% ACN/1% Trifluoroacetic acid (TFA) was added, and the mixture was shaken for 1 min, followed by sonication for 10 minutes. The supernatant was then removed and combined with the first one that was recovered earlier. Next, 35 µl of 100% ACN was added to the gel bands, and the mixture was shaken for 1 min, followed by sonication for 10 min. After that, the supernatant was removed and combined with the previous ones. Finally, all recovered supernatants were dried in a speedvac for 1 h or more at 30°C in V-AQ mode.

2.5 nanoLC-MS/MS Analytical Conditions

Peptide digests (1 µg) were injected and the samples were concentrated on a C18 cartridge (Dionex Acclaim Pep-Map100, 5 µm, 300 µm i.d. x 5 mm) and eluted on a capillary reverse-phase column (nanoEase M/Z Peptide CSH C18 Column, 130 A, 1.7 µm, 75 µmX 250 mm) at 220 nL/min, with a gradient of 2% to 40% of buffer B in45 min (A: 0.1% aq. FA/ACN 98:2 (v/v); B: 0.1% aq. FA/ACN 10:90 (v/v)), coupled to a quadrupole-Orbitrap mass spectrometer (Q Exactive HF, ThermoFisher

https://doi.org/10.5194/egusphere-2026-2192
Preprint. Discussion started: 20 May 2026

Scientific) using a Top 20 data-dependent acquisition MS experiment: 1 survey MS scan (400–2.000 m/z; resolution 70,000) followed by 20 MS/MS scans on the 20 most intense precursors (dynamic exclusion of 30 s, resolution 17,500).

2.6 Bioinformatic analysis

For LC-MS/MS data, protein identifications were performed using PEAKS® X-Pro software (64 bits version, 2020, Bioinformatics Solutions Inc, Canada). This software enables to search protein database via "*de novo*" approach. Protein sequences were downloaded from uniport (www.uniport.org, download date 10/07/2024) and following parameters were used for protein identification: MS and MS/MS tolerance: 10 ppm and 0.02 Da, respectively; enzyme: trypsin; fixed modification: carbamidomethylation; variable modification: oxidation of methionine. False discovery rate was < 1%. At least two unique peptides were required for a valid protein match.

2.7 FIB, STXM and TEM

A focused ion beam (FIB) ultrathin section was extracted from the wall of a test of a living specimen of *Ammonia confertitesta* using a FEI Strata DB 235 (IEMN, Lille, France) at low Ga-ion current to minimize mixing of components, creation of vacancies or amorphous layers, local compositional changes, or redeposition of the sputtered material on the sample surface (Bernard et al. 2009; Schiffbauer e Xiao 2009; Wirth 2009). Scanning transmission X-ray microscopy (STXM) and X-ray absorption near edge structure (XANES) data were collected using the HERMES STXM beamline at the synchrotron SOLEIL (Belkhou et al. 2015; Swaraj et al. 2017). Energy calibration was done using the well-resolved 3p Rydberg peak of gaseous CO2 at 294.96 eV for the C K-edge. X-ray absorption near edge structure (XANES) hypercube data (stacks) were collected at energy increments of 0.1 eV over the carbon (270–350 eV) absorption range with a dwell time of ≤ 1 ms per pixel to prevent irradiation damage (Wang et al. 2009). Stack alignments and extraction of XANES spectra were done using the free and open-source Python code Hyperspy (Pena et al. 2017). Using the method described in (Le Guillou et al. 2018), background was subtracted using a power law before spectra were normalized to the carbon quantity by integrating the spectra up to the mean ionization energy of carbons (e.g., up to 291.5 eV at the C K edge). High-resolution transmission electron microscopy (HRTEM) and scanning transmission electron microscopy (STEM) observations were performed on FIB foils with the 200 kV JEOL 2100F microscope operating at IMPMC (Paris, France), equipped with a field emission gun. Energy dispersive X-ray (EDX) spectra were acquired to probe the chemical composition, with a focused electron beam (1 nm) and a detection limit close to 0.1wt%.

3 Results

3.1 Extraction protocol of foraminiferal membrane-associated proteins and Annexin detection

We have developed and optimized an integrated protein extraction protocol capable of isolating three distinct protein fractions—total, soluble, and membrane-associated proteins—from a single extraction procedure.

https://doi.org/10.5194/egusphere-2026-2192
Preprint. Discussion started: 20 May 2026

Following (Betti et al. 2021), we modified the extraction buffer composition, with particular attention to optimizing the homemade lysis buffer (HM). To enhance the efficiency and reproducibility of the protocol, the HM buffer composition was simplified by reducing the number of components, retaining SDS as the sole detergent, and incorporating a commercial Protease Inhibitor Cocktail. This adjustment eliminated the need for manual addition of individual protease inhibitors, thereby streamlining preparation and minimizing sample-to-sample variability. The selected components ensured effective protein solubilization and protection, resulting in a formulation compatible with downstream applications such as immunoblotting. The protocol's effectiveness was further improved by implementing ultrasonic treatment, which induces cavitation bubble formation (Santos et al. 2008). This step proved particularly important for processing the exceptionally resilient cellular material tightly bound within foraminiferal tests.

The application of the protocol to 200 live specimens of *Ammonia* spp. revealed protein bands visualized by Coomassie Blue staining (Fig. 1a, 1b). The presence of distinct bands corresponding to total, soluble, and membrane-associated proteins clearly demonstrates the successful fractionation as hypothesized. Notably, soluble and membrane-associated proteins exhibit distinct qualitative and quantitative patterns.

Immunoblotting using an anti-Annexin A13 antibody, selected due to its documented presence in *R. filosa*, detected protein bands at ~36 kDa in both total and membrane-associated protein fractions (Fig. 1c), consistent with the expected size of Annexin A13. No signal was observed in the soluble fraction.

https://doi.org/10.5194/egusphere-2026-2192
Preprint. Discussion started: 20 May 2026

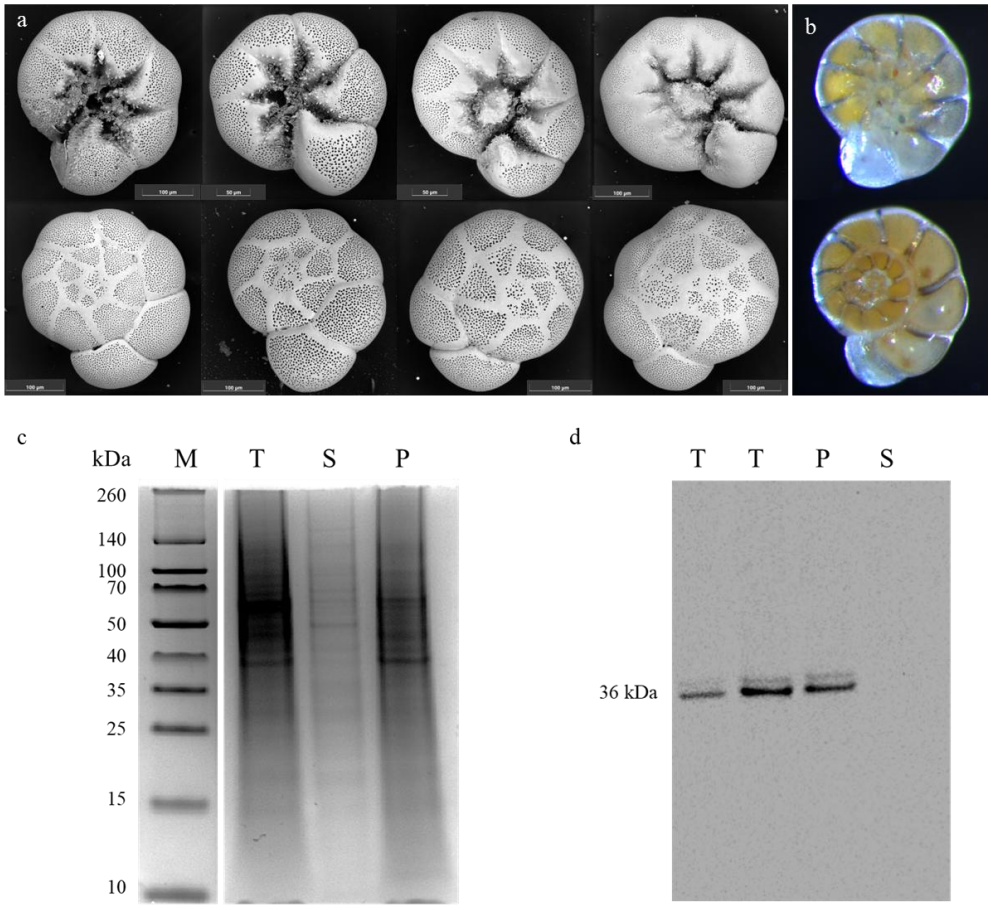

Figure 1: (a) Scanning electron microscopy (SEM) images of the most abundant *Ammonia* spp. specimens. (b) Stereomicroscope images (*Leica M165C*) of living *Ammonia* spp. specimens, showing the characteristic yellow–brown cytoplasm. (c) Coomassie Blue–stained 12% SDS–polyacrylamide gel showing total, soluble, and plasma membrane–associated protein fractions extracted from *Ammonia* spp. Protein extraction was performed from 200 individuals using 200 µL of extraction buffer per sample. (d) Western blot probed with anti-Annexin-13 antibody using the same fractions, revealing a band at ~36 kDa in total and membrane-associated protein fractions. M, standard molecular weight markers (SMW); T, total proteins; S, soluble proteins; P, plasma membrane–associated proteins. Gel and membrane images were processed for graphical purposes; original, unprocessed images are provided in the Fig. S1 (Supplements).

3.2 Proteomic characterization of foraminiferal proteins

Proteomic analysis of total, membrane-associated, and soluble protein fractions extracted from 500 foraminiferal specimens was performed using NanoLC-MS. Data analysis was conducted with PEAKS Xpro (Bioinformatics Solutions Inc.). To reduce uncertainty in protein identification, common contaminants such as keratins and proteins identified by only a single peptide were excluded.

https://doi.org/10.5194/egusphere-2026-2192
Preprint. Discussion started: 20 May 2026

The resulting protein data were cross-referenced with the Universal Protein (UniProt) database, with a particular focus on foraminiferal protein entries. Identified proteins (Table S1, Supplements) were classified according to functional annotations from the Gene Ontology (GO) database, ensuring precise grouping based on biological processes, cellular components, and molecular functions. By comparing these proteins to foraminiferal entries in UniProt, we gained deeper insights into their roles in key cellular processes, such as biomineralization, transport, and structural organization in foraminifera. Table 1 summarizes the principal proteins identified in the samples by NanoLC–MS, together with their functional classification, assigned according to the biological roles reported in the corresponding literature.

https://doi.org/10.5194/egusphere-2026-2192
Preprint. Discussion started: 20 May 2026

226 **Table 1: Main proteins identified in this study by NanoLC–MS and their functional classification, based on literature evidence**
227 **documenting their presence in foraminifera.**

Functional group (derived)	Main identified proteins in this study	Literature evidence
Calcium homeostasis	serine/threonine-protein phosphatases	(Ujiié et al. 2023; Prada et al. 2024)
	calcineurin	
	14-3-3-like protein	
Ions homeostasis	Na^+/K^+-exchanging ATPase	
	sodium/potassium-transporting ATPase subunit alpha-2	(Prada et al. 2024)
	V-type ATPase	(Sabbatini et al. 2014; Ujiié et al. 2023; Prada et al. 2024)
	H^+-transporting two-sector ATPase	(Sabbatini et al. 2014)
	H^+-exporting diphosphatases	
	Proton-translocating NAD(P)($^+$) transhydrogenase	
Vesicle formation	Polyubiquitin	(Prada et al. 2024)
	Clathrin heavy chain	(Prada et al. 2024)
	Heat Shock Protein 70	
	Heat Shock Protein 90	(Sabbatini et al. 2014)
	Rab2/RabB-family GTPase	
	Rab1/RabD-family GTPase	
ATP production	proton-translocating NAD(P)($^+$) transhydrogenase	
	ATP synthase beta subunit	
	ADP/ATP translocase	(Ujiié et al. 2023)
	succinate-CoA ligase	
	isocitrate dehydrogenase	
	aconitase/3-isopropylmalate dehydratase	
	dihydrolipoamide dehydrogenase	
Cytoskeleton dynamic	actin isoforms 1 and 2	(Sabbatini et al. 2014; Ujiié et al. 2023; Prada et al. 2024)
	α and β-tubulin	(Sabbatini et al. 2014; Ujiié et al. 2023; Prada et al. 2024)
	Rab7	(Stuhr et al. 2021)
	kinesins	
	calponin homology domain-containing protein	
Proteases	MPN domain-containing protein	
	ERAP1-like C-terminal domain	
	puromycin-sensitive aminopeptidase	

https://doi.org/10.5194/egusphere-2026-2192
Preprint. Discussion started: 20 May 2026

3.3 STEM and STXM characterization of the POS

The primary organic sheet (POS) of the terminal chamber wall of the *Ammonia confertitesta* specimen investigated is distinctly visible on SEM images obtained from a freshly fractured sample (Fig. 2a). This organic layer corresponds to the POS described by (Nagai, Uematsu, Wani, et al. 2018) and likely aligns with the P-, S-, and N-enriched layers identified in foraminiferal walls by (Branson et al. 2016; Geerken et al. 2019; Cisneros-Lazaro et al. 2022, 2024). The TEM characterization of a FIB section extracted from this wall (Fig. 2b) reveals that the POS comprises an irregular network of thin organic laminae oriented parallel to the test surface. This network forms a discontinuous, double-layered structure, appearing dark on images collected in STEM-HAADF mode (Fig. 2c).

While the bulk of the test wall consists of carbonate material—characterized by a XANES spectrum with a dominant peak at 290.3 eV and a broad feature around 300 eV, consistent with 1s→π* and 1s→σ* transitions of carbons in carbonate groups (Fig. 2d)—the POS is distinctly organic. Its XANES spectrum displays a main absorption at 288.6 eV, attributed to carboxylic carbons (1s→π*), a shoulder at 287.5 eV corresponding to aliphatic carbons bonded to hydrogen (1s→3p/σ*), and a peak at 285 eV indicative of aromatic or olefinic (C=C) carbons (1s→π*) (Fig. 4d - Le Guillou et al. 2018). The feature at 290.3 eV likely arises from the close association with carbonates at the nanoscale. This spectral signature, dominated by carboxylic and aliphatic carbons, is consistent with lipidic compounds, which are key constituents of cellular membranes.

Furthermore, the analysis of the organic residue remaining after EDTA extraction of the test reveals additional molecular species not spatially associated with the POS. XANES spectra of some of these compounds show features at 288.2 eV (amide groups), 287.1 eV (phenolic or ketonic groups), 289.5 eV (hydroxyl groups), and 285–285.5 eV (olefinic/aromatic carbons), collectively consistent with proteins or peptides (Fig. 2d). A second group of molecules exhibits absorption peaks at the same energies - excluding the 288.2 eV peak – but with different intensities and is more consistent with saccharidic structures (Fig. 2d).

https://doi.org/10.5194/egusphere-2026-2192
Preprint. Discussion started: 20 May 2026

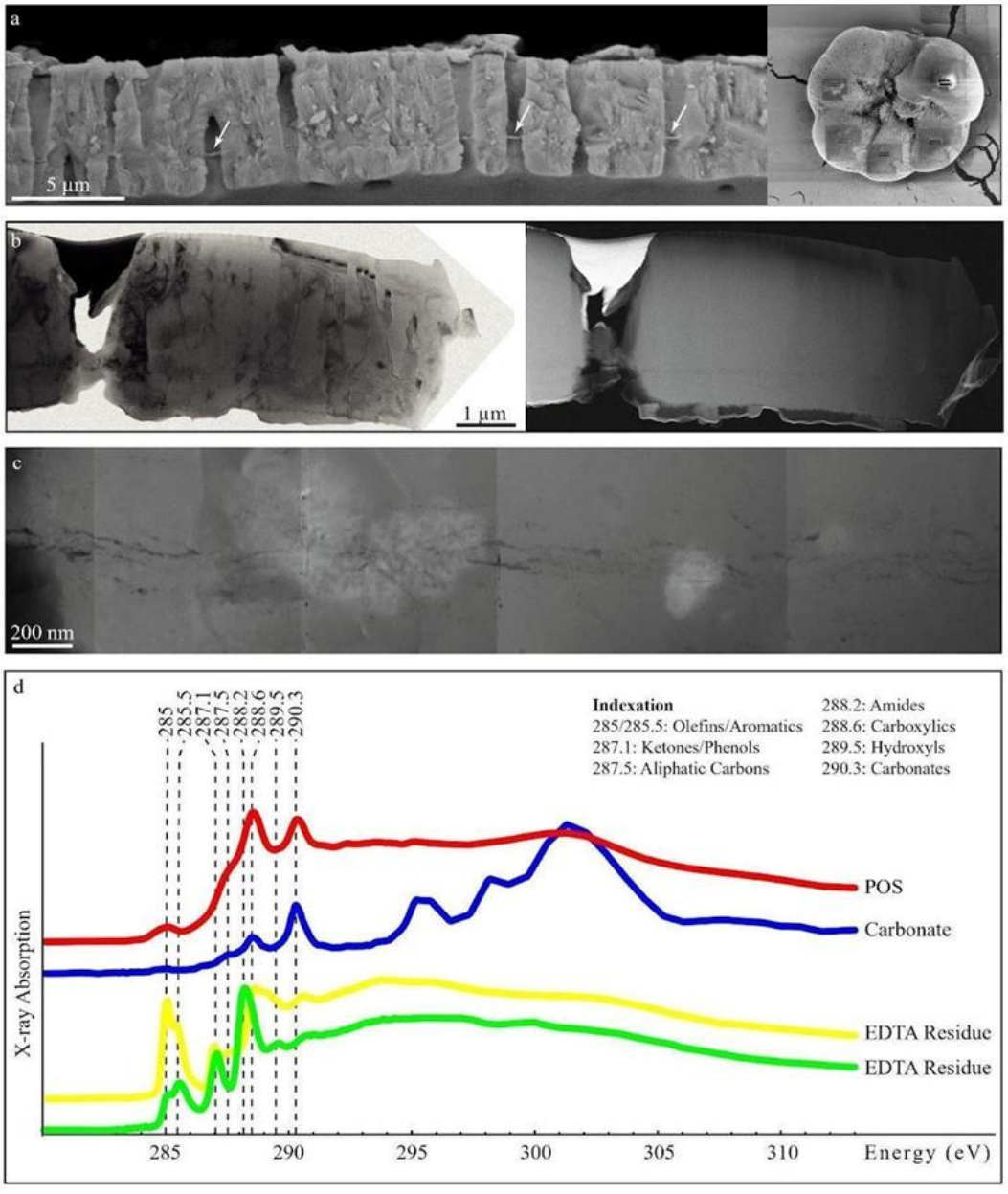

Figure 2: (a) SEM image of a freshly fractured chamber wall of a specimen of *Ammonia confertitesta* showing the POS (arrows). (b) TEM and STEM images of a FIB foil extracted over the entire wall of the last chamber of the specimen of *Ammonia confertitesta* shown in (a). (c) Mosaic of STEM images (HAADF mode) of the FIB foil shown in (b) showing the POS in dark, forming a discontinuous, double-layered structure. (d) XANES spectra of the POS and the carbonate matrix of the FIB section shown in (b), compared to the XANES spectra of organic residues after EDTA extraction. Indexation of peaks are given at the top right.

https://doi.org/10.5194/egusphere-2026-2192
Preprint. Discussion started: 20 May 2026

4 Discussion

4.1 Isolation of membrane-associated proteins including Annexin in foraminifera

In organisms lacking specialized calcifying tissues, such as unicellular foraminifera, functional differentiation must be interpreted at the subcellular level, particularly with regard to distinct cellular compartments and structures. The detection of membrane-associated proteins is of paramount importance to address questions regarding their possible role in biomineralization. Although their direct involvement in foraminiferal biomineralization has not yet been demonstrated, they are strong candidates for mediating critical processes such as intracellular vesicular transport of amorphous calcium carbonate (ACC), ion trans-membrane transport, and signal transduction, all of which may influence calcification (Erez 2003; de Nooijer et al., 2009; Toyofuku et al. 2017; Neherke et al. 2013; van Dijk et al. 2017; Dubicka et al. 2023, 2025). To address these questions at the molecular level, our protein extraction protocol was specifically developed to enable the separation of membrane-associated from soluble proteins, which is crucial for interpreting their potential involvement in biomineralization processes. In this framework, our results highlight the protocol's efficacy, not only in isolating proteins present in low quantities but also in clearly distinguishing membrane-associated and soluble protein fractions.

Among the membrane-associated proteins, the identification of Annexin A13 is particularly noteworthy, given its well-established role in calcium-dependent vesicular trafficking and Golgi-derived vesicle exocytosis in other eukaryotic systems (Gerke et al. 2005).

From a broader evolutionary and functional perspective, annexins are widely conserved across eukaryotes (Einarsson et al. 2016). Annexins are Ca^{2+}- and lipid-binding proteins involved in calcium transport and can function as ion channels within Matrix Vesicles (MVs) (Hasegawa et al. 2017). They participate in diverse intracellular processes, such as vesicle-mediated transport, signalling, and membrane–cytoskeleton interactions. More recently, (Grewal et al. 2025) revisited the role of annexins, confirming their implication in membrane-related events along endo- and exocytic pathways and strongly highlighting their role as key regulators of membrane trafficking. Consistent with this conserved role, the presence of Annexin A13 in foraminiferal genomic data and its annotated sequence in UniProt (UniProtKB X6LBI7) suggests that annexins are also present in marine benthic foraminifera. Due to their calcium-dependent binding to acidic membrane phospholipids, annexins may play a role in directing calcium to foraminiferal biomineralization sites, supporting test formation and calcium carbonate deposition. We investigated annexin-like proteins via Western blot analysis, confirming for the first time the presence of annexin family proteins in membrane-associated protein fractions of foraminiferal extracts. This observation is consistent with the hypothesis that membrane-associated proteins, such as members of the annexin family, may contribute to the regulation of calcium delivery to sites of biocalcification. However, functional studies are required to directly test this still speculative hypothesis. In this context, the role of annexins as membrane calcium-transporting proteins could be complementary to the presence of transmembrane calcium ion channels identified through proteomic analyses by Prada et al. (2024), as well as to the transmembrane calcium transport mechanism to the site of biocalcification hypothesized by Nehrke et al. (2013).

https://doi.org/10.5194/egusphere-2026-2192
Preprint. Discussion started: 20 May 2026

4.2 Fraction-Resolved Proteomic Analysis and Potential Implications for Biomineralization

Biological interpretation of the proteomic data was performed as described by (Prada et al. 2024). However, our study extends this framework by examining, rather than only proteins from the organic shell matrices, the entire cellular proteome, including the separation of the total protein extract into its two main components: soluble and membrane-associated fractions. The qualitative analysis of these fractions provided insights into the subcellular localization of proteins, an essential aspect for advancing our understanding of their functional roles.

In the following sections, we discuss the main functions of the proteins identified in this study in light of their potential involvement in foraminiferal biocalcification (Table 1). Although the functional annotations of these proteins are primarily derived from the literature, we emphasize the significance of their detection in foraminifera and the complementary perspective that our proteomic approach provides with respect to existing models of foraminiferal calcification, which have so far mainly focused on mineralogical and chemical mechanisms (Erez 2003; Bentov et al., 2009; de Nooijer et al., 2009; Neherke et al. 2013; Dubicka et al. 2023, 2025). In particular, we propose that various groups of membrane-associated proteins may act in coordination to regulate calcium availability and control the chemical microenvironment of the calcification site, while other proteins involved in intracellular metabolic pathways could provide the necessary energetic support for these processes.

Chamber formation in foraminifera requires precise Ca^{2+} homeostasis (~100 nM at rest) to prevent cytotoxicity (Berridge et al. 2000), yet the molecular mechanisms underlying this process remain poorly understood. Our study reveals the presence of serine/threonine-protein phosphatases in *Ammonia* species. The detection of these enzymes confirms calmodulin-dependent phosphatase activity, mediating the calcium-regulated dephosphorylation of serine/threonine residues. This finding is particularly significant because previous studies have identified calcium/calmodulin-dependent protein kinases in *Ammonia beccarii* (Ujiié et al. 2023) and *Amphistegina lobifera* (Prada et al. 2024), which are involved in Ca^{2+}-mediated signalling during biomineralization.

Our results gain further relevance in light of the well-established roles of calmodulin and calmodulin-like proteins in the regulation of Ca^{2+} transport and vesicular secretion. In addition, our analysis identified calcineurin, a highly conserved protein across eukaryotes (Creamer, 2020), which is activated in response to elevated intracellular calcium levels.

Calmodulin and calcineurin interact to form an active phosphatase complex. This complex plays a crucial role in various cellular processes, including the regulation of calcium-release channels, such as ryanodine receptors, and the modulation of the microtubule-associated protein tau (Creamer 2020).

We also identified the 14-3-3-like protein, which is well known for its role in cell signaling and protein-protein interactions. Dedman et al. (2024) further demonstrated that a highly acidic 14-3-3 domain is conserved across biocalcifying algae reinforcing its proposed role in biomineralization through calcium-binding capabilities and regulatory functions. Building upon the role of calcium homeostasis in calcification, Prada et al. (2024) highlighted the importance of solute carrier proteins in regulating calcification fluid composition, identifying these transporters within the shell organic matrices. We show that the same key ion transporters, including the Na^+/K^+-exchanging ATPase and its alpha-2 subunit, previously implicated in *Mytilus*

https://doi.org/10.5194/egusphere-2026-2192
Preprint. Discussion started: 20 May 2026

edulis larval development (Ramesh et al., 2019), are enriched in the membrane-associated protein fraction. This localization suggests that they operate at the cellular level to mediate ion exchange and regulate calcification fluid composition, and that they function at the plasma membrane before ultimately being incorporated or detected within the shell organic matrices.

In our study, we identified several proteins associated with vesicles formation, consistent with previous findings by Prada et al. (2024). Notably, we detected polyubiquitin and the clathrin heavy chain, indicating that clathrin-mediated endocytosis may play a central role in the initial stages of vesicles formation. The importance of vesicle formation and its involvement in biocalcification was first suggested by Erez (2003), Bentov et al., (2009) and de Nooijer et al. (2009; 2014), and has since been further emphasised by Dubicka et al. (2023, 2025). In particular, the latter documented in symbiotic rotaliid *Amphistegina lobifera* the intracellular production of Mg-rich ACC that is stored in large vesicles. This suggests that intracellular ACC might serve as a precursor phase for the formation of calcite shells, providing strong evidence in support of an intracellular biocalcification pathway (Dubicka et al. 2023, 2025).

In addition, we identified Heat Shock Protein 70 and Heat Shock Protein 90, both known to facilitate clathrin uncoating during vesicle maturation (Kaksonen & Roux 2018). Multiple Rab-family GTPases, including Small Rab-related GTPase, Rab2/RabB-family GTPase, and Rab1/RabD-family GTPase were also identified. They are involved in regulating protein secretion, exocytosis, and vesicle docking, primarily by facilitating the initial tethering between vesicles.

Finally, we confirmed the presence of key cytoskeletal components, a particularly noteworthy discovery is the identification of Rab7, a Ras-related GTPase known to coordinate cytoskeletal dynamics with intracellular signaling, especially in vesicle trafficking and membrane remodeling (Stuhr et al. 2021). Additionally, we detected kinesins, motor proteins that likely transport mineral-loaded vesicles along microtubules toward sites of calcification (Lee & Liu 2004), a vesicular transport mechanism previously described in foraminifera by Dubicka et al. (2023, 2025). Their membrane association suggests a role in organizing the cytoskeletal architecture at the calcification front, potentially explaining the precise morphological control observed during chamber formation.

4.3 Molecular Signatures and Functional Interpretation of the POS

SEM and TEM observations of the last chamber wall of *Ammonia confertitesta* reveal a distinct Primary Organic Sheet (POS) forming a discontinuous organic network parallel to the test surface (Fig. 2a–c). It is believed that the POS structure plays a vital role in rotaliid biocalcification, serving as a template for the deposition of calcium carbonate on both sides and resulting in the bilayer structure of the last chamber wall (inner and outer calcitic layers). It was first named the Primary Organic Membrane (POM) in pioneering works (e.g. Hemleben et al., 1986). Erez (2003) subsequently proposed changing this terminology to 'primary organic sheet' (POS), considering it to be an “extracellular organic matrix”. The POS has then described as a sheet of spongy organic material between the inner and outer calcitic layers (Hottinger 1986), high enriched in P, S, Na and N (Branson et al. 2016; Geerken et al. 2019, Cisneros Lazaro et al. 2022, 2024). Subsequent structural and ultrastructural studies have refined this view, demonstrating that the cross-section of a newly forming chamber wall exhibits a “sandwich” architecture, with active cytoplasmic pseudopodia coating both sides of the POS, where calcite nucleation is

https://doi.org/10.5194/egusphere-2026-2192
Preprint. Discussion started: 20 May 2026

initiated (Nagai, Uematsu, Chen, et al. 2018; Nagai, Uematsu, Wani, et al. 2018; Tyszka et al. 2019). More recently, (Sancho Vaquer et al. 2025) interpreted the microstructure of the POS in the rotaliid *Neogloboquadrina dutertrei* as an extensive network of biopolymer fibrils forming the previously described spongy organic material. This fibrillar framework is proposed to function as the calcite nucleation template, with crystallites forming directly within the POS structure. In this context, XANES analyses clearly distinguish the carbonate-dominated test wall from the POS, which exhibits a predominantly organic molecular signature dominated by carboxylic, aliphatic, and olefinic/aromatic carbons, consistent with lipid-rich compounds (Fig. 3d; Le Guillou et al. 2018), reflecting the presence of lipidic molecules that are key constituents of cellular membranes. In addition, organic residues remaining after EDTA decalcification reveal molecular components consistent with proteins or peptides, as well as saccharidic structures, which are not spatially associated with the POS. Based on this multidisciplinary dataset, we propose that the POS represents an organic layer likely derived at least in part from the plasma membrane. In fact, the discontinuous nanoscale organization of the POS, together with its lipid-dominated molecular signature identified by *in situ* X-ray synchrotron analyses, supports a membrane-related origin rather than a solely pre-formed extracellular matrix (Nagai, Uematsu, Chen, et al. 2018; Nagai, Uematsu, Wani, et al. 2018). We hypothesize that these lipid signatures represent remnants of membrane-associated macromolecules that played a templating role during calcium carbonate precipitation. In other biocalcifying organisms, organic matrices are typically composed of proteins, glycoproteins, and polysaccharides (Weiner & Addadi 1997), which exert tight control over the morphology and properties of the growing inorganic–organic composite. Angell (1967) described a fibrous “basal membrane” located between the IOL and the basal calcareous lamella, consisting of a protein–polysaccharide complex. More recently, (Sabbatini et al. 2014) identified acid-soluble N-glycoproteins and sugar moieties, including high-mannose-type glycans and other carbohydrates, within the organic layers of rotaliid foraminifera, including the POS.

Once their function was accomplished, these macromolecules likely became entrapped within the calcite, forming the discontinuous organic layer reported in the literature. The possibility that the POS retains traces of membrane lipids and may therefore derive from the plasma membrane shifts attention toward a potentially significant, yet often overlooked, role of the plasma membrane in biomineralization, underscoring the need for its detailed characterization.

5 Conclusions

Our proteomic data highlight the involvement of several proteins in the internalisation of seawater via endocytosis. This process likely occurs through a clathrin-mediated mechanism, followed by the sequestration of calcium into intracellular vesicles and then its transport to the plasma membrane for targeted release at biocalcification sites. The detection Annexin A13, suggests its possible role in calcium-dependent vesicle docking to the calcification site. Together with the identification of proteins involved in vesicular trafficking, such as clathrin, Rab GTPases, and polyubiquitin, these molecular findings support the presence of a specialized vesicular network regulating intracellular calcium transport during chamber formation. This mechanism may complement the active one through plasma membrane active transporters.

https://doi.org/10.5194/egusphere-2026-2192
Preprint. Discussion started: 20 May 2026

Our multidisciplinary approach further suggests that the Primary Organic Sheet (POS) represents a vestige of the plasma membrane. Nanoscale imaging and in situ XANES spectroscopy revealed lipid signatures and a discontinuous organic network within the POS, consistent with a membrane-derived origin. Although the plasma membrane itself cannot become part of the shell, membrane-derived lipids and proteins may be released during biomineralization and subsequently trapped within the calcite structure. In this way, the shell preserves molecular traces of membrane-associated components that likely contribute to the organization and templating of the POS, providing new insights that complement existing biomineralization models in foraminifera.

Code and Data availability

The mass spectrometry proteomics data have been deposited to the ProteomeXchange Consortium via the PRIDE partner repository with the dataset identifier PXD069533 (DOI: 10.6019/PXD069533). During peer review, the data can be accessed via PRIDE using the reviewer credentials:
Username: reviewer_pxd069533@ebi.ac.uk
Password: xCTaTcxrlrLr
The dataset will be made publicly available upon publication.

Supplements

Fig. S1. Unprocessed images of protein analyses from *Ammonia* spp. (a) Original Coomassie Blue–stained 12% SDS–polyacrylamide gel showing total, soluble, and plasma membrane–associated protein fractions. (b) Original Western blot probed with anti-Annexin-13 antibody, showing a band at ~36 kDa in total and membrane-associated protein fractions.
Table S1. Comprehensive Protein Annotation Dataset. The datasets are provided as Excel files. This table includes all proteins identified in the analyzed protein fractions: cytoplasmic, membrane-associated, and total extracts. The presence of each protein in a given fraction is indicated by an “x” in the corresponding column. Proteins are functionally classified into groups based on Gene Ontology (GO) terms. For each protein, we provide the UniProt accession number, the name under which the protein is deposited in the UniProt database, the molecular functions it performs, the biological processes in which it is involved, and the cellular compartment in which it has been localized, according to information retrieved from UniProt.

Author contributions

A.S., A.B., F.Z. and E.C. Conceptualization; E.C., F.Z., A.M. and S.B. Investigation; A.B., A.M., S.B. and F.Z. Resources; E.C., A.M. and S.B. Formal analysis; and A.S. and E.C. Writing (original draft preparation). A.S., A.B., F.Z., S.B., A.M. and E.C. Writing (review and editing).

https://doi.org/10.5194/egusphere-2026-2192
Preprint. Discussion started: 20 May 2026

Competing interests

The authors declare that they have no conflict of interest.

Acknowledgements

This work was supported by the Italian Ministry of University and Research (MUR) under the PRIN 2020 program (Prot. 2020EEMH5R), Project Title: bIogeochemiCal fate of emerging Anthropogenic pollutants in the sedimentary Record: a model based on foraminifEra (ICare); CUP: I33C20014370001.

We acknowledge financial support under the National Recovery and Resilience Plan (NRRP), Mission 4, Component 2, Investment 1.1, Call for tender No. 1628 published on 16.10.2020 by the Italian Ministry of University and Research (MUR), funded by the European Union – NextGenerationEU – Project Title: MeChanisms Of carbonate biomineraLizatiOn driVen by selected unicEllular oRganisms under Stress conditions. CO2 Lovers – CUP Master: F53C24001060006 – CUP UNIVPM: I53C24002640006.

This project was produced while attending the PhD programme in PhD in Sustainable Development And Climate Change at the University School for Advanced Studies IUSS Pavia, Cycle XXXVIII, with the support of a scholarship financed by the Ministerial Decree no. 351 of 9th April 2022, based on the NRRP - funded by the European Union - NextGenerationEU - Mission 4 "Education and Research", Component 1 "Enhancement of the offer of educational services: from nurseries to universities" - Investment 4.1 "Extension of the number of research doctorates and innovative doctorates for public administration and cultural heritage".

Artificial Intelligence was used in this doctoral thesis to support the proofreading of the English language.

Financial support

This open-access publication was funded by the Italian Ministry of University and Research (MUR) under the PRIN 2020 program (Prot. 2020EEMH5R), Project Title: bIogeochemiCal fate of emerging Anthropogenic pollutants in the sedimentary Record: a model based on foraminifEra (ICare); CUP: I33C20014370001.

Review statement

The review statement will be added by Copernicus Publications listing the handling editor as well as all contributing referees according to their status anonymous or identified.

https://doi.org/10.5194/egusphere-2026-2192
Preprint. Discussion started: 20 May 2026

References

Angell, R. W. (1967). The Test Structure and Composition of the Foraminifer Rosalina floridana. The Journal of Protozoology—Wiley Online Library. https://doi.org/10.1111/j.1550-7408.1967.tb02001.x

Angell, R. W. (1979). Calcification during chamber development in Rosalina floridana. Journal of Foraminiferal Research, 9(4), 341–353. https://doi.org/10.2113/gsjfr.9.4.341

Angell, R. W. (1980). Test morphogenesis (chamber formation) in the foraminifer Spiroloculina hyalina Schulze. Journal of Foraminiferal Research, 10(2), 89–101. https://doi.org/10.2113/gsjfr.10.2.89

Banner, F. T., Sheehan, R., & Williams, E. (1973). The organic skeletons of rotaline foraminifera; a review. Journal of Foraminiferal Research, 3(1), 30–42. https://doi.org/10.2113/gsjfr.3.1.30

Bañuelos, S., Saraste, M., & Carugo, K. D. (1998). Structural comparisons of calponin homology domains: Implications for actin binding. Structure, 6(11), 1419–1431. https://doi.org/10.1016/S0969-2126(98)00141-5

Bè, A. W. H., Hemleben, C., Anderson, O. R., & Spindler, M. (1979). Chamber Formation in Planktonic Foraminifera. Micropaleontology, 25(3), 294–307. https://doi.org/10.2307/1485304

Belkhou, R., Stanescu, S., Swaraj, S., Besson, A., Ledoux, M., Hajlaoui, M., & Dalle, D. (2015). HERMES: A soft X-ray beamline dedicated to X-ray microscopy. Journal of Synchrotron Radiation, 22(4), 968–979. https://doi.org/10.1107/S1600577515007778

Bentov, S., Brownlee, C., & Erez, J. (2009). The role of seawater endocytosis in the biomineralization process in calcareous foraminifera. Proceedings of the National Academy of Sciences, 106(51), 21500–21504. https://doi.org/10.1073/pnas.0906636106

Bernard, S., Benzerara, K., Beyssac, O., Brown, G. E., Stamm, L. G., & Duringer, P. (2009). Ultrastructural and chemical study of modern and fossil sporoderms by Scanning Transmission X-ray Microscopy (STXM). Review of Palaeobotany and Palynology, Spore/pollen fine structure in living and fossil plants, 156(1), 248–261. https://doi.org/10.1016/j.revpalbo.2008.09.002

Berridge, M. J., Lipp, P., & Bootman, M. D. (2000). The versatility and universality of calcium signalling. Nature Reviews Molecular Cell Biology, 1(1), 11–21. https://doi.org/10.1038/35036035

Betti, M., Ciacci, C., Abramovich, S., & Frontalini, F. (2021). Protein Extractions from Amphistegina lessonii: Protocol Development and Optimization. Life, 11(5), 418. https://doi.org/10.3390/life11050418

Branson, O., Bonnin, E. A., Perea, D. E., Spero, H. J., Zhu, Z., Winters, M., Hönisch, B., Russell, A. D., Fehrenbacher, J. S., & Gagnon, A. C. (2016). Nanometer-Scale Chemistry of a Calcite Biomineralization Template: Implications for Skeletal Composition and Nucleation. Proceedings of the National Academy of Sciences, 113(46), 12934–12939. https://doi.org/10.1073/pnas.1522864113

Caridi, F., Sabbatini, A., Birarda, G., Costanzi, E., De Giudici, G., Galeazzi, R., Medas, D., Mobbili, G., Ricciutelli, M., Ruello, M. L., Vaccari, L., & Negri, A. (2020). Cigarette butts, a threat for marine environments: Lessons from benthic foraminifera (Protista). Marine Environmental Research, 162, 105150. https://doi.org/10.1016/j.marenvres.2020.105150

https://doi.org/10.5194/egusphere-2026-2192
Preprint. Discussion started: 20 May 2026

Cisneros-Lazaro, D., Adams, A., Guo, J., Bernard, S., Baumgartner, L. P., Daval, D., Baronnet, A., Grauby, O., Vennemann, T., Stolarski, J., Escrig, S., & Meibom, A. (2022). Fast and pervasive diagenetic isotope exchange in foraminifera tests is species-dependent. Nature Communications, 13(1), 113. https://doi.org/10.1038/s41467-021-27782-8

Cisneros-Lazaro, D., Adams, A., Stolarski, J., Bernard, S., Daval, D., Baronnet, A., Grauby, O., Baumgartner, L. P., Vennemann, T., Moore, J., Baumgartner, C., Martin Olmos, C., Escrig, S., & Meibom, A. (2024). Fossil biocalcite remains open to isotopic exchange with seawater for tens of millions of years. Scientific Reports, 14(1), 24933. https://doi.org/10.1038/s41598-024-75588-7

Creamer, T. P. (2020). Calcineurin. Cell Communication and Signaling, 18(1). https://doi.org/10.1186/s12964-020-00636-4

de Nooijer, L. J., Toyofuko, T., & Kitazato, H. (2009). Foraminifera promote calcification by elevating their intracellular pH | PNAS. Recuperato 24 febbraio 2026, da https://www.pnas.org/doi/abs/10.1073/pnas.0904306106

de Nooijer, L. J., Spero, H. J., Erez, J., Bijma, J., & Reichart, G. J. (2014). Biomineralization in perforate foraminifera. Earth-Science Reviews, 135, 48–58. https://doi.org/10.1016/j.earscirev.2014.03.013

Dedman, C. J., Chauhan, N., González-Lanchas, A., Baldreki, C., Dowle, A. A., Larson, T. R., Lee, R. B. Y., & Rickaby, R. E. M. (2024). Exploring proteins within the coccolith matrix. Scientific Reports, 14(1), 31821. https://doi.org/10.1038/s41598-024-83052-9

Dubicka, Z., Bojanowski, M. J., Bijma, J., & Bickmeyer, U. (2023). Mg-rich amorphous to Mg-low crystalline CaCO3 pathway in foraminifera. Heliyon, 9(7). https://doi.org/10.1016/j.heliyon.2023.e18331

Dubicka, Z., Syczewski, M. D., Benning, L. G., Schreiber, A., Wirth, R., Witkowski, M., Bojanowski, M. J., Pałczyńska, A., Janse, M., & Bickmeyer, U. (2025). Amorphous calcium carbonate loaded multilamellar vesicles within Amphistegina (Rotaliida) foraminifera. Acta Biomaterialia, 208, 525–537. https://doi.org/10.1016/j.actbio.2025.10.060

Dubicka, Z., Tyszka, J., Pałczyńska, A., Höhne, M., Bijma, J., Jense, M., Klerks, N., & Bickmeyer, U. (2024). Biocalcification in porcelaneous foraminifera. eLife, 13, RP91568. https://doi.org/10.7554/eLife.91568

Einarsson, E., Ástvaldsson, A., Hultenby, K., Andersson, J. O., Svärd, S. G., & Jerlström-Hultqvist, J. (2016,). Comparative Cell Biology and Evolution of Annexins in Diplomonads. mSphere. https://doi.org/10.1128/msphere.00032-15

Erez, J. (2003). The Source of Ions for Biomineralization in Foraminifera and Their Implications for Paleoceanographic Proxies. Reviews in Mineralogy and Geochemistry, 54(1), 115–149. https://doi.org/10.2113/0540115

Fehrenbacher, J. S., Hupp, B. N., Branson, O., Evans, D., Foster, G. L., Glock, N., Thirumalai, K., & Wycech, J. (2024). INDIVIDUAL FORAMINIFERAL ANALYSES: A REVIEW OF CURRENT AND EMERGING GEOCHEMICAL TECHNIQUES. Journal of Foraminiferal Research, 54(4), 312–331. https://doi.org/10.61551/gsjfr.54.4.312

Geerken, E., de Nooijer, L. J., Roepert, A., Polerecky, L., King, H. E., & Reichart, G. J. (2019). Element banding and organic linings within chamber walls of two benthic foraminifera. Scientific Reports, 9(1), 3598. https://doi.org/10.1038/s41598-019-40298-y

Gerke, V., Creutz, C. E., & Moss, S. E. (2005). Annexins: Linking Ca2+ signalling to membrane dynamics. Nature Reviews. Molecular Cell Biology, 6(6), 449–461. https://doi.org/10.1038/nrm1661

Glas, M. S., Langer, G., & Keul, N. (2012). Calcification acidifies the microenvironment of a benthic foraminifer (Ammonia sp.). Journal of Experimental Marine Biology and Ecology, 424–425, 53–58. https://doi.org/10.1016/j.jembe.2012.05.006

Grewal, T., Gerke, V., Nylandsted, J., Rentero, C., & Enrich, C. (2025). Revisiting the role of Annexins in membrane trafficking. Cellular and Molecular Life Sciences, 82(1), 230. https://doi.org/10.1007/s00018-025-05780-z

Hasegawa, T., Yamamoto, T., Tsuchiya, E., Hongo, H., Tsuboi, K., Kudo, A., Abe, M., Yoshida, T., Nagai, T., Khadiza, N., Yokoyama, A., Oda, K., Ozawa, H., de Freitas, P. H. L., Li, M., & Amizuka, N. (2017). Ultrastructural and biochemical aspects of matrix vesicle-mediated mineralization. Japanese Dental Science Review, 53(2), 34–45. https://doi.org/10.1016/j.jdsr.2016.09.002

Hemleben, C., Be, A. W. H., Anderson, O. R., & Tuntivate, S. (1977). Test morphology, organic layers and chamber formation of the planktonic foraminifer Globorotalia menardii (d'Orbigny). Journal of Foraminiferal Research, 7(1), 1–25. https://doi.org/10.2113/gsjfr.7.1.1

Hottinger. (1986). Construction, structure and function of foraminiferal shells. (Oxford University Press, New York).

Kaksonen, M., & Roux, A. (2018). Mechanisms of clathrin-mediated endocytosis. Nature Reviews Molecular Cell Biology, 19(5), 313–326. https://doi.org/10.1038/nrm.2017.132

Katz, M. E., Cramer, B. S., Franzese, A., Hönisch, B., Miller, K. G., Rosenthal, Y., & Wright, J. D. (2010). TRADITIONAL AND EMERGING GEOCHEMICAL PROXIES IN FORAMINIFERA. Journal of Foraminiferal Research, 40(2), 165–192. https://doi.org/10.2113/gsjfr.40.2.165

Le Guillou, C., Bernard, S., De la Pena, F., & Le Brech, Y. (2018). XANES-Based Quantification of Carbon Functional Group Concentrations. Analytical Chemistry, 90(14), 8379–8386. https://doi.org/10.1021/acs.analchem.8b00689

Lee, Y.-R. J., & Liu, B. (2004). Cytoskeletal Motors in Arabidopsis. Sixty-One Kinesins and Seventeen Myosins. Plant Physiology, 136(4), 3877–3883. https://doi.org/10.1104/pp.104.052621

Nagai, Y., Uematsu, K., Chen, C., Wani, R., Tyszka, J., & Toyofuku, T. (2018). Weaving of biomineralization framework in rotaliid foraminifera: Implications for paleoceanographic proxies. Biogeosciences, 15(22), 6773–6789. https://doi.org/10.5194/bg-15-6773-2018

Nagai, Y., Uematsu, K., Wani, R., & Toyofuku, T. (2018). Reading the Fine Print: Ultra-Microstructures of Foraminiferal Calcification Revealed Using Focused Ion Beam Microscopy. Frontiers in Marine Science, 5. https://doi.org/10.3389/fmars.2018.00067

Nehrke, G., Keul, N., Langer, G., de Nooijer, L. J., Bijma, J., & Meibom, A. (2013). A new model for biomineralization and trace-element signatures of Foraminifera tests. Biogeosciences, 10(10), 6759–6767. https://doi.org/10.5194/bg-10-6759-2013

Pavard, J. C., Richirt, J., Seuront, L., Blanchet, H., Fouet, M. P., Humbert, S., Gouillieux, B., Duong, G., & Bouchet, V. M. (2023). The great shift: The non-indigenous species Ammonia confertitesta (Foraminifera, Rhizaria) outcompetes indigenous Ammonia species in the Gironde estuary (France). Estuarine, Coastal and Shelf Science, 289, 108378. https://doi.org/10.1016/j.ecss.2023.108378

Pawlowski, J., & Holzmann, M. (2002). Molecular phylogeny of Foraminifera a review. European Journal of Protistology, 38(1), 1–10. https://doi.org/10.1078/0932-4739-00857

de la Pena, F. , Ostasevicius, T. , Fauske, V. , Burdet, P. , Jokubauskas, P. , Nord, M. , Sarahan, M. , Prestat, E. , Taillon, J. , Caron, J. , Furnival, T. , MacArthur, K. , Eljarrat, A. , Mazzucco, S. , Migunov, V. , Aarholt, T. , Walls, M. , Winkler, F. , Donval, G. , Martineau, B. , Garmannslund, A. , Zagonel, L., & Iyengar, I. (2017). Electron microscopy (big and small) data

https://doi.org/10.5194/egusphere-2026-2192
Preprint. Discussion started: 20 May 2026

analysis with the open source software package HyperSpy. Microscopy and Microanalysis, 23(S1), 214-215. https://doi.org/10.1017/S1431927617001751

Prada, F., Haramaty, L., Livnah, O., Shaul, R., Abramovich, S., Mass, T., Rosenthal, Y., & Falkowski, P. G. (2024). Proteomic characterization of a foraminiferal test's organic matrix. Proceedings of the National Academy of Sciences, 121(50), e2417845121. https://doi.org/10.1073/pnas.2417845121

Ramesh, K., Yarra, T., Clark, M. S., John, U., & Melzner, F. (2019). Expression of calcification-related ion transporters during blue mussel larval development. Ecology and Evolution, 9(12), 7157–7172. https://doi.org/10.1002/ece3.5287

Robbins, L. L., & Donachy, J. E. (1991). Mineral Regulating Proteins from Fossil Planktonic Foraminifera. Surface Reactive Peptides and Polymers (Vol. 444, pp. 139–148). American Chemical Society. https://doi.org/10.1021/bk-1991-0444.ch010

Sabbatini, A., Bédouet, L., Marie, A., Bartolini, A., Landemarre, L., Weber, M. X., Gusti Ngurah Kade Mahardika, I., Berland, S., Zito, F., & Vénec-Peyré, M.-T. (2014). Biomineralization of Schlumbergerella floresiana, a significant carbonate-producing benthic foraminifer. Geobiology, 12(4), 289–307. https://doi.org/10.1111/gbi.12085

Sancho Vaquer, A., Griesshaber, E., Meilland, J., Fernández-Díaz, L., Yin, X., Lastam, J., de Nooijer, L., Kucera, M., & Schmahl, W. W. (2025). Microstructure and Texture of Foraminiferal Ca-Carbonate: The Different Biomineralization Strategies of Rotaliida, Robertinida, and Miliolida. Crystal Growth & Design, 25(10), 3274–3297. https://doi.org/10.1021/acs.cgd.4c01531

Santos, H. M., Lodeiro, C., & Capelo-Martínez, J.-L. (2008). The Power of Ultrasound. In Ultrasound in Chemistry (pp. 1–16). John Wiley & Sons, Ltd. https://doi.org/10.1002/9783527623501.ch1

Schiebel, R., & Hemleben, C. (2017). Ecology. In R. Schiebel & C. Hemleben (A c. Di), Planktic Foraminifers in the Modern Ocean (pp. 209–230). Springer. https://doi.org/10.1007/978-3-662-50297-6_7

Schiffbauer, J. D., & Xiao, S. (2009). Novel application of focused ion beam electron microscopy (FIB-EM) in preparation and analysis of microfossil ultrastructures: A new view of complexity in early Eukaryotic organisms. PALAIOS, 24(9), 616–626. https://doi.org/10.2110/palo.2009.p09-003r

Spero, H. J. (1988). Ultrastructural examination of chamber morphogenesis and biomineralization in the planktonic foraminiferOrbulina universa. Marine Biology, 99(1), 9–20. https://doi.org/10.1007/BF00644972

Stuhr, M., Cameron, L. P., Blank-Landeshammer, B., Reymond, C. E., Doo, S. S., Westphal, H., Sickmann, A., & Ries, J. B. (2021). Divergent Proteomic Responses Offer Insights into Resistant Physiological Responses of a Reef-Foraminifera to Climate Change Scenarios. Oceans, 2(2), Articolo 2. https://doi.org/10.3390/oceans2020017

Sun, X., Yang, A., Wu, B., Zhou, L., & Liu, Z. (2015). Characterization of the Mantle Transcriptome of Yesso Scallop (Patinopecten yessoensis): Identification of Genes Potentially Involved in Biomineralization and Pigmentation. PLOS ONE, 10(4), e0122967. https://doi.org/10.1371/journal.pone.0122967

Swaraj, S., Belkhou, R., Stanescu, S., Rioult, M., Besson, A., & Hitchcock, A. P. (2017). Performance of the HERMES beamline at the carbon K-edge. Journal of Physics: Conference Series, 849(1), 012046. https://doi.org/10.1088/1742-6596/849/1/012046

Toyofuku, T., Matsuo, M. Y., de Nooijer, L. J., Nagai, Y., Kawada, S., Fujita, K., Reichart, G.-J., Nomaki, H., Tsuchiya, M., Sakaguchi, H., & Kitazato, H. (2017). Proton pumping accompanies calcification in foraminifera. Nature Communications, 8(1), 14145. https://doi.org/10.1038/ncomms14145

https://doi.org/10.5194/egusphere-2026-2192
Preprint. Discussion started: 20 May 2026

Toyofuku, T., Suzuki, M., Suga, H., Sakai, S., Suzuki, A., Ishikawa, T., de Nooijer, L. J., Schiebel, R., Kawahata, H., & Kitazato, H. (2011). Mg/Ca and δ18O in the brackish shallow-water benthic foraminifer Ammonia 'beccarii'. Marine Micropaleontology, 78(3), 113–120. https://doi.org/10.1016/j.marmicro.2010.11.003

Tyszka, J., Bickmeyer, U., Raitzsch, M., Bijma, J., Kaczmarek, K., Mewes, A., Topa, P., & Janse, M. (2019). Form and function of F-actin during biomineralization revealed from live experiments on foraminifera. Proceedings of the National Academy of Sciences, 116(10), 4111–4116. https://doi.org/10.1073/pnas.1810394116

Tyszka, J., Godos, K., Goleń, J., & Radmacher, W. (2021). Foraminiferal organic linings: Functional and phylogenetic challenges. Earth-Science Reviews, 220, 103726. https://doi.org/10.1016/j.earscirev.2021.103726

Ujiié, Y., Ishitani, Y., Nagai, Y., Takaki, Y., Toyofuku, T., & Ishii, S. (2023). Unique evolution of foraminiferal calcification to survive global changes. Science Advances, 9(25), eadd3584. https://doi.org/10.1126/sciadv.add3584

Urey, H. C., Lowenstam, H. A., Epstein, S., & McKinney, C. R. (1951). Measurement of paleotemperatures and temperatures of the Upper Cretaceous of England, Denmark, and the southeastern United States. Geological Society of America Bulletin, 62(4), 399-416. https://doi.org/10.1130/0016-7606(1951)62[399:MOPATO]2.0.CO;2

van Dijk, I., de Nooijer, L. J., & Reichart, G.-J. (2017). Trends in element incorporation in hyaline and porcelaneous foraminifera as a function of pCO_2. Biogeosciences, 14(3), 497–510. https://doi.org/10.5194/bg-14-497-2017

Veschi, E. A., Bolean, M., Strzelecka-Kiliszek, A., Bandorowicz-Pikula, J., Pikula, S., Granjon, T., Mebarek, S., Magne, D., Ramos, A. P., Rosato, N., Millán, J. L., Buchet, R., Bottini, M., & Ciancaglini, P. (2020). Localization of Annexin A6 in Matrix Vesicles During Physiological Mineralization. International Journal of Molecular Sciences. https://doi.org/10.3390/ijms21041367

Wang, J., Morin, C., Li, L., Hitchcock, A. P., Scholl, A., & Doran, A. (2009). Radiation damage in soft X-ray microscopy. Journal of Electron Spectroscopy and Related Phenomena, Radiation Damage, 170(1), 25–36. https://doi.org/10.1016/j.elspec.2008.01.002

Weiner, S., & Addadi, L. (1997). Design strategies in mineralized biological materials. Journal of Materials Chemistry, 7(5), 689–702. https://doi.org/10.1039/A604512J

Weiner, S., & Dove, P. M. (2003). An Overview of Biomineralization Processes and the Problem of the Vital Effect. Reviews in Mineralogy and Geochemistry, 54(1), 1–29. https://doi.org/10.2113/0540001

Wirth, R. (2009). Focused Ion Beam (FIB) combined with SEM and TEM: Advanced analytical tools for studies of chemical composition, microstructure and crystal structure in geomaterials on a nanometre scale. Chemical Geology, Accessory minerals as tracers of crustal processes, 261(3), 217–229. https://doi.org/10.1016/j.chemgeo.2008.05.019

Yang, J., Zhao, Z., Gu, M., Feng, X., & Xu, H. (2019). Release and uptake mechanisms of vesicular Ca2+ stores. Protein & Cell, 10(1), 8–19. https://doi.org/10.1007/s13238-018-0523-x